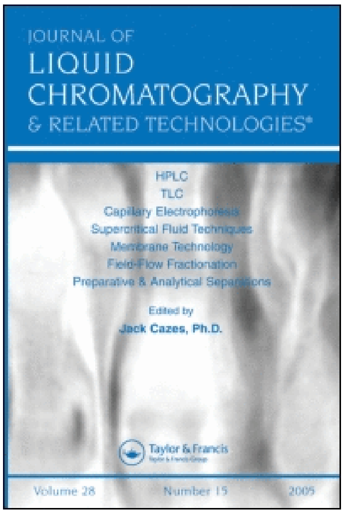

Journal of Liquid Chromatography & Related Technologies
Publication details, including instructions for authors and subscription information:
http://www.informaworld.com/smpp/title~content=t713597273

Preparation of Various Bonded Phases for HPLC Using Monochlorosilanes

Gert E. Berendsen[a]; Krijn A. Pikaart[a]; Leo de Galan[a]
[a] Laboratory for Analytical Chemistry Delft, University of Technology, Delft, The Netherlands

To cite this Article Berendsen, Gert E. , Pikaart, Krijn A. and de Galan, Leo(1980) 'Preparation of Various Bonded Phases for HPLC Using Monochlorosilanes', Journal of Liquid Chromatography & Related Technologies, 3: 10, 1437 — 1464

To link to this Article: DOI: 10.1080/01483918008062788

URL: http://dx.doi.org/10.1080/01483918008062788

JOURNAL OF LIQUID CHROMATOGRAPHY, 3(10), 1437-1464 (1980)

PREPARATION OF VARIOUS BONDED PHASES FOR HPLC USING MONOCHLOROSILANES

Gert E. Berendsen, Krijn A. Pikaart and Leo de Galan
Laboratory for Analytical Chemistry
Delft University of Technology
Jaffalaan 9, 2628 BX Delft
The Netherlands

ABSTRACT

Monochlorosilanes have been prepared with yields of about 80% through a catalytic hydrosilylation of terminal olefins. Subsequently, the silanes are chemically bonded to silica to obtain: (i) n-octyldimethylsilyl bonded phases with reproducible surface coverage ranging from 0.8 to 3.5 μmol/m^2, (ii) propyldimethylsilyl bonded phases with different functional groups at the γ-position, all showing a nearly equal surface coverage of some 3.3 μmol/m^2, and (iii) n-alkyldimethylsilyl bonded phases with chainlengths ranging from 1 to 22 carbon atoms and with surface coverages ranging from 3.9 μmol/m^2 for RP-1 to 3.0 μmol/m^2 for the RP-22 bonded phase. A simplified model based on the pore structure of silica allows an explanation and estimation of the maximum surface coverage as a function of the chainlength of the bonded phase.

INTRODUCTION

In previous publications |1,2| we have advocated the use of monochlorosilanes for the preparation of reproducible and well defined chemically bonded phases for liquid chromatography. From a geometrical model based on molecular dimensions we concluded that the maximally attainable surface coverage of silica approximated 4 μmol/m^2 or 2.4 chains/nm^2. From this model an impression could be given about the screening of remaining hydroxyl groups by the bonded phase |1|. In a consecutive paper |2| we described the preparation of some short-chain bonded phases and the minor influence of residual silanol groups on retention. The present paper reports the preparation of a variety of chemically bonded phases derived from monochlorosilanes.

Although the preparation of chemically bonded phases has been described in many papers most attention has been paid to dichloro- and trichlorosilanes [3-15], whereas only a few studies report the use of monochloro compounds [1,2, 16-19].

Although in either case the extent of the bonding reaction can be expressed by the carbon content of the end product, we agree with Unger [20] and Colin and Guiochon [21] that the carbon percentage is a poor measure of the surface coverage of the packing material. The conversion of the carbon percentage to the more significant surface coverage can only be made reliably for monochlorosilanes [2] and even then only when the properties of the starting silicas are known. As long as the respective influences of surface coverage, the nature of the bonded phase and the remaining silanol groups, are not quantitatively established one should be careful in comparing retention data of clearly different covered phases. Hence the data of Hemetsberger et al. [10,11,15], who studied the influence of chainlength of bonded alkyl chains at maximum surface coverage, are not directly comparable with those of Hennion et al.[13], who studied this effect at constant, but less than maximum coverage (i.e. 2.1 umol/m^2). In our opinion, conclusions on optimum chain length [12] and optimized preparation conditions [14] are premature if they are based on studies using decidedly undercovered phases. In fact, a mutual comparison of different chain lengths prepared from mono-, di- and trichlorosilanes is only justified, if the influence of remaining hydroxyl groups at constant surface coverage and chain length is taken into account [17].

EXPERIMENTAL

Chemicals used for the preparation of the bonded packings were obtained from different sources. Silanes from Petrarch Systems (Levittown, Penna., US), except trimethylchlorosilane (Aldrich); olefins mainly from Fluka, and Aldrich; the catalyst hexachloroplatinum(IV)acid-hexahydrate from Drijfhout, Amsterdam, The Netherlands.

All bonded packings were prepared from batches of LiChrosorb SI 100 silica of Merck. Two batches of 10 um particles (batch nr. EF 72 with charge nr. 527.1302, and batch nr. EH 23, charge nr. 854.6446), and one batch of 5 um particles (batch nr. EH 2, charge nr. 632.2712).

The specific surface areas of the three batches were determined in duplicate with the BET nitrogen adsorption method at 77K |22| as 299 m^2/g for batch EF 72, 313 m^2/g for EH 23 and 273 m^2/g for the 5 μm particles, batch EH 2. A gas expansion apparatus was used with gauged volumes.

Pore structure parameters such as specific pore volume, pore size distribution and mean pore size were obtained from the nitrogen adsorption isotherm according to the cylindrical model discussed by De Boer |23|, Broekhoff |24| and Linsen |25|. The isotherms were obtained with a Sorptomatic model 1826, Carlo Erba, Milan, Italy.

Elemental analysis of carbon, hydrogen and, if present, chlorine or nitrogen, were performed under dry nitrogen in two independent laboratories. The data were converted to true surface coverages using the expression derived previously |2|.

$$N\ (\mu mol/m^2) = \frac{10^6 \cdot P_C}{1200 n_C - P_C(M-1)} \cdot \frac{1}{S} \qquad (1)$$

where P_C is the measured carbon percentage, S the specific surface area (in m^2/g), M the molecular weight of the bonded molecule and n_C the number of carbon atoms in the bonded silane molecule. In eq. (1) the factor $P_C(M-1)$ corrects for the weight increase of the silica. A similar expression can be formulated for other elements, but for hydrogen the contribution of remaining silanol groups must be taken into account |2|.

Thermogravimetry - Mass Spectrometry measurements were performed with a combined TG-DTA-EGA apparatus of Satorius, coupled to a Topatron-B mass spectrometer of Leybold-Heraeus. Some 50 mg sample was heated at a rate of 6 K/min under vacuum or in helium (20 mL/min). Weight loss and heat change were recorded continuously, and the evolved gases were fed into the ionization chamber of the mass spectrometer, that could be triggered to record a 10 s mass spectrum every minute.

PREPARATION OF CHEMICALLY BONDED PACKINGS

Preparation of a chemically bonded stationary phase involves surface modification of a porous silica support by chemical reaction of silanol groups with an appropriate silane reagent.

As has been discussed previously |1| there are enough active silanol groups available. Surface pretreatment with strong acids in order to increase this number |2,13| is unnecessary and not advisable, because this treatment may introduce possible structural changes in the silica support |2|. Moreover, additional silanol groups will not enhance the surface coverage, but may reduce the nonpolar character of the bonded packing.

The dimethylmonochlorosilane reagent ($ClSi(CH_3)_2$-R) can be synthesized in several ways. Unger et al. |16| used a two-step Grignard reaction.

$$(1)\quad C_nH_{2n+1}\text{-}Br \;+\; Mg \longrightarrow C_nH_{2n+1}MgBr$$

$$(2)\quad C_nH_{2n+1}MgBr \;+\; (CH_3)_2SiCl_2 \longrightarrow \underset{\text{monomer}}{C_nH_{2n+1}Si(CH_3)_2Cl}$$

The obvious possibility of dimer formation adversely affects the reaction yield.

We used a rapid and simple one-step catalytic hydrosilylation of terminal olefins for the preparation of monochloro- and monoalkoxysilanes. This reaction favours the formation of an "anti-Markovnikov"-addition product. A review of various hydrosilylation reactions is given by Seyferth and King |26|.

$$R\text{-}(CH_2)_m\text{-}CH{=}CH_2 \;+\; (CH_3)_2ClSiH \xrightarrow{\text{catalyst}} R\text{-}(CH_2)_{m+2}Si(CH_3)_2Cl$$

inwhich R=H or functional group. The catalyst used was hexachloroplatinum-acid-hexahydrate ($H_2PtCl_6.6H_2O$). In general, this reaction type involves shorter reaction times and higher yields in comparison with the Grignard reaction type |27|. Note that only functional groups can be used which do not react with the monochloro- or monoalkoxysilanes. Other functional groups, viz. -OH, must be protected by socalled "protecting groups" which have to be removed after the bonding reaction.

The preparation of monochlorosilanes proceeds under reflux and in a dry nitrogen atmosphere.

To 0.2 mole olefin add about 2 mg hexachloroplatinumacid-hexahydrate catalyst. Heat the solution under continuous stirring to a temperature of 90°C (except the olefin 1-hexene (boiling point 63.5°C); this solution was heated to 50°C). Add an equivalent (or small excess) of dimethylchlorosilane in about 30-40 min. The reaction is highly exothermic as is shown by an increase in temperature.

To prevent overheating the reactionvessel is cooled. The dimethylmonochlorosilane product is purified by fractional distillation under vacuum and stored in sealed glass ampoules. The yields of the synthesized monochlorosilane products are presented in table I.

Some monochlorosilanes with various terminal functional groups are commercially available, i.e. Cl-$Si(CH_3)_2$-$(CH_2)_3$-X, inwhich X=H, CN or Cl; and CH_3O-Si

TABLE I

Yields and physical properties of monochlorosilanes

silane compound $X-(CH_2)_n-Si(CH_3)_2Cl$ X	n	boiling and melting points (°C) bp/mm Hg	mp	YIELD (%)
H	6	65-67/12.5		82
	10	130-133/15		84
	14	152-153/2		84
	18	182-185/0.2	*25-30*	82
	22	-	*40-45*	66
phenyl	3	∿65/12.5§)		77
cyclohexyl	3	∿65/12.5§)		64
dimethylamine	3	-		80§§)
vinyl	3	52-54/18		38§§§)

§) *boiling points are difficult to define due to excessive foaming*

§§) *the salt formed during reaction of the dimethylamine with dimethylchlorosilane is removed by filtering the final solution*

§§§) *for complications with this synthesis, see references /28/ and /29/*

$(CH_3)_2-(CH_2)_3-CH_2NH_2$ with a reactive methoxy group instead of a chlorine atom. Some other silanes were synthesized from their corresponding olefins (i.e. $CH_2=CH_2CH_2-X$, inwhich X= phenyl, cyclohexyl, dimethylamine and vinyl). Obviously, silanes from olefins with cyanide or halogen terminal functional groups can also be easily prepared. Tabel I presents data of silane compounds with functional groups.

Proton NMR-Spectroscopy (60 MHz) is eminently suitable to follow the conversion of the olefin into the monochlorosilane compound. Vanishing of the signals from olefinic hydrogens at δ=4.6-5.9 ppm is accompanied by the appearance of a singlet at δ=0.41 ppm arising from methylgroups bonded to the silicon atom. The methylene groups, except the one directly bonded to the silicon atom, cause a sharp signal at δ=1.30 ppm. The silicon bonded methylene group and the terminal methylgroup (for n-alkyl chains) give rise to a complex signal between δ=0.60 and δ=1.17 ppm.

The spectra of monochlorosilanes with functional groups all show a distorted 2-proton triplet at $\delta=0.95$ ppm for the methylene group bonded to silicon. Chemical shifts of the other methylene groups (a multiplet and a triplet) depend upon the functional group. Similar results have been found by Mourey and Siggia |30|.

Synthesis of bonded packings

Various chemically bonded materials were prepared from three different silica batches. One batch was used for preparing packings with different chain lengths, another for preparing both different chain lengths and undercovered phases, and a third one for synthesizing short chain phases with various terminal functional groups.

Bonded packings with different n-alkyl chain lengths were prepared using a revised version of the bonding reaction described previously |2|.

The bonding reaction is carried out in a dry atmosphere. To a mixture of 100 ml toluene (dried over sodium), 4 gram silica (activated for 12 hours at 200°C and ∿1.5 torr) and 2.5 ml pyridine (dried over KOH) a four fold excess of silane reagent (calculated for 2.4 silanol groups per nm^2) is added. This mixture is heated for 40-150 hours (depending on chainlength) at a temperature about 10°C below the boiling point of the most volatile component. Occasionally, the mixture is gently stirred or shaken with care to prevent damaging of the particles. The bonded packing was washed as described previously |2| and dried for 12 hours at 150°C in vacuo, before samples were taken for the elemental analysis.

Except for some RP-3, RP-10 and RP-18 materials, which were only used for test purposes, all bonded packings were post-treated with trimethylchlorosilane in the same way as described above.

Undercovered phases were prepared from n-octyldimethylchlorosilane at roomtemperature. Appropriate amounts of silane reagent (calculated on the basis of 2.4 silanol groups per nm^2) were added to the mixture of toluene, pyridine and silica. All manipulations and reactions were carried out in a glove box, filled with absolutely dry nitrogen. The reaction time was one week.

The short chain phases with various terminal functional groups were also synthesized at roomtemperature with a reaction time of one week, but with a four fold excess of silane reagent. Actually, this reaction time is excessive. According to Van de Venne |19|, a maximum coverage with n-octyldimethylsilane is realized slightly over four hours. For aminobutyldimethylmonomethoxysilane we followed the bonding procedure as described for trimethylmonoethoxysilane, using activated silica and N,N-dimethylaniline as reaction-stimulant |2|.

After washing |2| and drying (at 150°C/1.5 torr for 12 hours), samples for the elemental analysis were taken under dry nitrogen and stored in sealed glass ampoules.

RESULTS AND DISCUSSION

Surface coverage

Surface coverages of the bonded materials were calculated from the data of the elemental analysis using eq. (1) and are presented in table II.

Table II a and b show the results for n-alkylbonded phases of variable chain length. Apparently, the surface coverage decreases with increasing chain length from about 4 μmol/m^2 for RP-1 to about 3 μmol/m^2 for RP-22, the longest chain presently prepared. The maximum value of 3.9 μmol/m^2 obtained for an RP-1 packing, table II a, agrees with the value found previously |2| for TMS with another silica batch (EF 72, i.e. the same batch as used for packings in table II d). However, the RP-1 coverage in table II b (batch EH 2) is somewhat higher, 4.2 μmol/m^2. This difference appears to be systematic. For most RP-phases the surface coverage is a few percent higher on the EH-2 batch, despite the lower carbon percentage. This proves our previous statement that the carbon percentage is a poor measure to characterize chemically bonded phases, since it ignores the surface area of the silica eq. (1). The coverages presented in both tables are in excellent agreement with those published by Unger et al. |16|, who used a different bonding procedure at a much higher temperature (250° against 95°C). It is rather remarkable that these values appear not to have been reproduced in a later publication |17|.

In view of the uncertain correction applied to the hydrogen percentage |2|, the surface coverages obtained from the hydrogen percentage agree fairly well with those from the more reliable, corresponding carbon percentages.

With increasing chain length the surface coverage decreases and hence, the number of remaining silanol groups on the silica surfaces increases. In an attempt to cap some additional silanol groups, all n-alkyl bonded phases were post-treated with a large excess of trimethylchlorosilane (TMCS). However, as indicated in Table II a, the carbon and hydrogen percentage do not raise. If we assume, that post-treatment with TMCS would produce the same coverage (in chains per nm^2) for all phases, then the carbon percentage would have increased by 0.35% for RP-3, 0.51% for RP-10, and 0.92% for RP-18. Such changes would have been readily observed in the elemental analysis, which is precise to 0.1% absolute for these duplicate measurements. Consequently, we disagree with Karger et al. |18| that the carbon percentage is a poor and inaccurate measure of the effect of post-silanization.

Furthermore, the negative result of the elemental analysis is confirmed by chromatographic experiments. As has been found previously for short chain phases |2|, post-silanization of fully covered phases does not change the retention or peak shape of solutes measured under reversed phase conditions. The data for RP-10, presented in figure 1, are illustrative for all comparisons made. It can

TABLE II a

Surface coverages of n-alkylsilyl bonded phases
(silica support, EH 23, S_{BET}= 313 m^2/g, 10 μm particles)

MONOCHLORO SILANES $H-(CH_2)_n-Si(CH_3)_2Cl$	WEIGHT PERCENTAGES				SURFACE COVERAGE				DESIGNATION
	direct		after treatment with TMCS		mmol/g		μmol/m^2	nm^{-2}	
n	C	H	C	H	C	H			
1	4.01	1.29	—	—	1.21	1.24	3.87	2.33	RP-1
3	6.01	1.61	6.00	1.69	1.11	1.19	3.56	2.14	RP-3
6	9.23	1.92	8.99	2.03	1.10	1.03	3.51	2.11	RP-6
10	12.72	2.54	12.62	2.67	1.07	1.05	3.41	2.05	RP-10
14	15.51	3.30	15.63	3.39	1.02	1.15	3.26	1.97	RP-14
18	17.65	3.59	17.58	3.37	0.95	1.34	3.04	1.83	RP-18
22	20.03	3.68	20.03	3.95	0.93	1.35	2.98	1.80	RP-22

be concluded, therefore, that post-treatment with TMCS of fully covered silicas is unnecessary, at least for use under reversed phase conditions. A possible influence of post-silanization under straight phase conditions has not been investigated.

Table II c presents data of reversed phase (RP-8) packings with increasing surface coverage, prepared at roomtemperature. Figure 2 shows the relation between the expected surface coverage calculated from the added octylsilane and the coverage derived from elemental analysis. Evidently for coverages up to 2 μmol/m^2 all added silane reacts, whereas at higher concentrations the coverage is less than expected. It is remarkable, however, that even under such mild reaction conditions of roomtemperature and only 36% excess of silane a surface coverage of 3.28 μmol/m^2 is realized. This is only 5% less than the maximum coverage of 3.45 μmol/m^2 realized by reacting a four fold excess of silane at 95°C. The maximum coverage of 3.45 μmol/m^2 agrees with the coverage obtained for RP-8 on the same silica batch in table II b. Hence we agree with Van de Venne

TABLE II b

Surface coverages of n-alkylsilyl bonded phases
(silica support, EH 2, S_{BET} = 273 m^2/g, 5 µm particles)

MONOCHLORO SILANES $H-(CH_2)_n-Si(CH_3)_2Cl$	*WEIGHT PERCENTAGES*		*SURFACE COVERAGE*				DESIGNATION
			mmol/g		µmol/m^2	nm^{-2}	
n	C	H	C	H			
1	3.78	1.07	1.14	0.98	4.16	2.51	RP-1
3	5.32	1.39	0.97	0.97	3.56	2.15	RP-3
6	8.28	1.80	0.98	0.93	3.60	2.17	RP-6
8	9.84	2.09	0.95	0.94	3.49	2.10	RP-8
14	14.52	2.64	0.94	0.84	3.43	2.06	RP-14
18	16.83	2.99	0.90	0.81	3.28	1.97	RP-18

|19| that chemically bonded phases can be synthesized with a good reproducibility on the same silica support. A further indication for this reproducibility is the absence of scatter of the data points around the smooth curve in figure 2.

Finally, table II d presents results for propylsilyl bonded phases with different functional groups at the γ-position. All these phases show a nearly equal surface coverage of some 3.3 µmol/m^2, except the butylamino-phase, which shows a lower coverage of 2.4 µmol/m^2. However, the latter bonded packing was prepared from a monomethoxysilane compound and with activated silica. Apparently, the methoxy group is less reactive than the chlorine atom, as has also been found previously for trimethylsilane phases |2|.

The surface coverages calculated from the percentages of hydrogen and of the hetero-atoms are in acceptable agreement with those from the carbon percentages.

The coverage of 3.36 µmol/m^2 for the n-propylbonded phase prepared with a four fold excess at roomtemperature, is slightly less than the coverage of 3.56 µmol/m^2 for the RP-3 phase in table II a, prepared at 95°C with a similar

TABLE II c

n-Octyldimethylsilyl phase with increasing surface coverage (silica support, EH 2, S_{BET}≈ 273 m^2/g, 5 μm particles)

MONOCHLORO SILANES	*WEIGHT PERCENTAGES* C	H	*SURFACE COVERAGE* mmol/g C	H	μmol/m^2	nm^{-2}
$H-(CH_2)_8-Si(CH_3)_2Cl$	2.62	1.27	0.23	0.46	0.83	0.50
	5.27	1.38	0.47	0.52	1.74	1.05
	6.20	1.57	0.57	0.62	2.08	1.25
	7.64	1.77	0.71	0.74	2.62	1.58
	8.52	1.93	0.81	0.84	2.96	1.78
	9.32	2.06	0.90	0.92	3.28	1.97
	9.73	2.12	0.94	0.96	3.45	2.08

excess of silane. This small but significant difference is attributed to a change in reaction temperature rather than to a variation in the type of silica used. Indeed, the surface coverage for RP-1 in table II a agrees well with the value found previously for the same silica batch as used for phases in table II d, and treated at the same temperature |2|.

The surface coverages obtained under relatively mild conditions (i.e. 95°C in liquid environment) are equally high as those reported by Unger and Roumeliotis |17|, in their gas-phase reaction at 250°C *in vacuo*.

Structure of chemically bonded packings

Three chemically bonded phases (i.e. RP-3, RP-10 and RP-10, table II a), and the silica support itself, were selected for a study of the influence of chain length on specific surface area, pore volume, pore radius, pore distribution and pore shape. These data can be obtained from the complete isotherm of the adsorbed volume of nitrogen, V_a, expressed in ml gas NTP/g adsorbent, at 77 K as a function of the pressure between 0 and 1 atm (figure 3) |23|.

TABLE II d

Surface coverages of phases with terminal functional groups (silica support, EF 72, S_{BET}= 299 m^2/g, 10 µm particles)

BONDED SILANE MOIETY $X-(CH_2)_n-Si(CH_3)_2-$		WEIGHT PERCENTAGES			SURFACE COVERAGE				
					mmol/g			µmol/m²	nm⁻²
-X	n	C	H	N	C	H	N		
$-NH_2$	4	4.63	1.38	0.88	0.70	0.74	0.68	2.35	1.41
$-N(CH_3)_2$	3	6.89	2.08	1.09	0.93	1.20	0.88	3.11	1.87
-CN	3	6.43	1.25	1.29	0.99	0.89	1.03	3.32	2.00
-Cl	3	5.49	1.28	2.73§	1.04	0.95	0.86§	3.49	2.10
-H	3	5.48	1.55		1.01	1.10		3.36	2.03
-C=C	3	7.32	1.67		0.98	1.07		3.27	1.97
	3	10.66	2.12		0.35	0.95		3.17	1.91
	3	10.81	1.80		0.96	1.09		3.20	1.93

§ *value for chlorine*

The specific surface area, S_{BET}, is calculated from the volume of adsorbed nitrogen, v_m, which is required to cover a sample of (modified) silica with a unimolecular layer. This layer is realized at a relative pressure, p/p_o, of about 0.1, and is determined from the intercept and slope of the "BET-plot" measured between p/p_o of 0.05 and 0.30 [22].

After the unimolecular layer is completed, multimolecular layers are formed, and if the adsorbent is porous, capillary condensation will take place in the pores. The latter results in a strong increase of the adsorbed volume, V_a, and starts at a smaller p/p_o ratio, the smaller the pores are. This effect is indeed observed from the isotherms in figure 3. For longer bonded chain length, the pore radius decreases and the p/p_o ratio, where capillary condensation manifests itself, shifts to lower values. The start of the condensation is presented by the start of the hysteresis loop between p/p_o of 0.6 and 0.7, and decreases for longer chains.

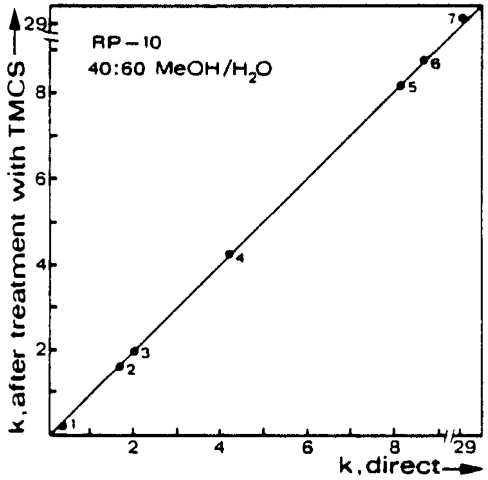

1. *acetone*
2. *p-methoxyphenol*
3. *phenol*
4. *m-cresol*
5. *anisole*
6. *3,5-xylenol*
7. *p-phenylphenol*

FIGURE 1

Constancy of retention on the RP-10 phase after post-treatment with TMCS

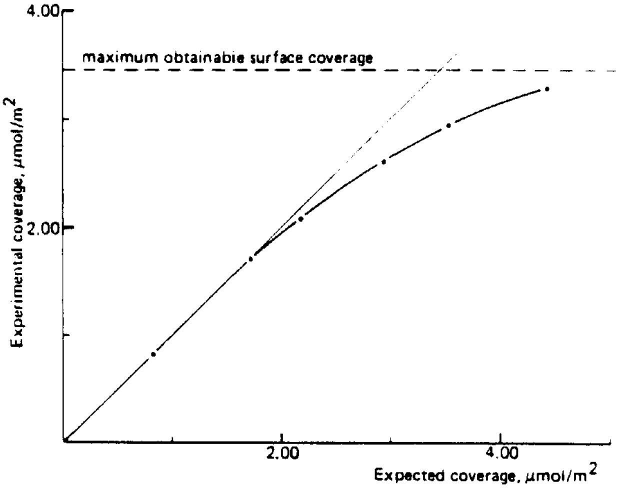

FIGURE 2

Difference between the predicted and obtained surface coverage of the undercovered RP-8 packings

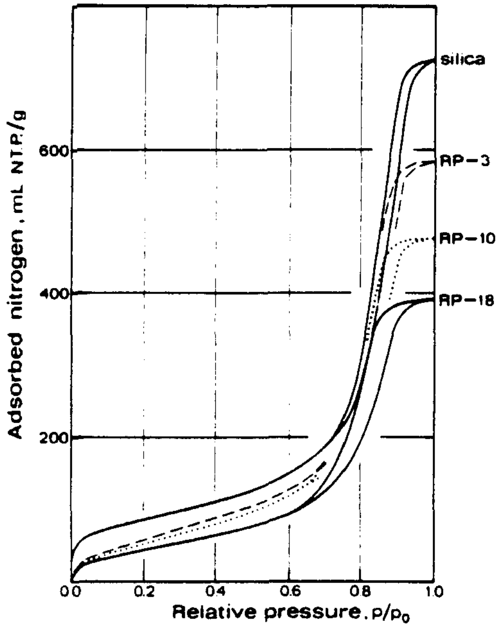

FIGURE 3
Nitrogen adsorption and desorption isotherms of three n-alkylsilyl bonded phases and of the silica support; discussion in the text

The other pore structure quantities, such as volume, radius and shape were obtained from the adsorption branch (i.e. the right-hand branch) of the hysteresis loop, according to the capillary condensation equation of Kelvin |23|. The left-hand branch presents the desorption branch. The shape of the hysteresis loop provides information on the pore shape |23|. When the two branches are parallel, as is observed in fig. 3 for pure silica, then the pores are cylindrically shaped. The non parallel branches observed for RP-18 indicate a tendency towards ink-bottle-shaped pores, possibly arising from clusters of RP-chains.

The average radius of the pores, R_p, can be obtained from the pore radius distribution curve. All four materials studied exhibit similar distribution curves, but the position of the curve maximum shifts to higher values with increasing chain length. The pore radii of the unmodified silica support vary from 3 to 12 nm, with an average value of 8.0 nm. For the longest chain studied, the RP-18 packing, the radii vary from 2 to 11 nm, and the average is reduced to 6.0 nm.

The absence of micropores smaller than 1 nm is concluded from the "t-method" described by De Boer and coworkers |31-33|. In this method the nitrogen adsorption isotherm obtained for a porous solid is compared with a standard isotherm corresponding with a nonporous solid of the same type.

The specific pore volume, V_p, is determined from the final part of the sorption isotherm when the relative pressure is close to unity. At this point pores are filled with liquid nitrogen.

The different pore parameters are presented in table III. The large discrepancy between the measured pore diameter of 16 nm, wh[illegible] sured in dupli for the original silica support, SI 100, and the di[illegible] 10 nm stated by Me is remarkable. The same deviation was observed by [illegible] Le Venne [19], who used mixture of three silica batches. For another silica (EH 2; V_p=1.15 ml/g), the measured radius of 8.7 nm also exceeds the nominal value of 5 nm.

Obviously, mutual comparison of specific surface areas and pore volumes is only possible after a correction of the primary data for the weight increase of

TABLE III

Pore structure parameters for some packing materials measured by nitrogen adsorption

DESIGNATION OF PACKING MATERIAL	R_p (nm)	MEASURED		CORRECTION FOR WEIGHT INCREASE	CORRECTED	
		S_{BET} m^2/g material	V_p ml/g material	(1+N(M-1)) (ref. 2)	S_{BET} m^2/g silica	V_p ml/g silica
ORIGINAL SILICA	8.0	313	1.10	—	313	1.10
RP-3	7.3	259	0.86	1.111	288	0.95
RP-10	6.6	220	0.72	1.212	267	0.87
RP-18	6.0	182	0.51	1.295	236	0.66

the modified silica |2|. This correction is shown in the fifth column of table III. It is not surprising that S_{BET}, V_p and R_p decrease with increasing chain length.

In agreement with the cylindrical shape of the pores the BET-surface decreases in direct proportionality with the measured pore radius, whereas the pore volume, V_p, decreases with the square of the pore radius. In fact, it is easily possible to convert the BET-surface and the pore volume to equivalent pore radii, using eq. (2).

$$\frac{R_{p,RP}}{R_{p,silica}} = \frac{S_{BET,RP}}{S_{BET,silica}} = \sqrt{\frac{V_{p,RP}}{V_{p,silica}}} \qquad (2)$$

These data are presented in table IV and demonstrates the consistency of the three independently measured pore parameters: R_p, S_{BET} and V_p. However, the data do not provide an insight in the position of the bonded chains on the silica surface. This is provided by the final two columns in table IV. Here, the pore radius for bonded packings is derived for two different models. In the last but one column it is assumed that the bonded phase is packed so closely that it resembles a liquid of hydrocarbons physically coated onto the surface. The thick-

TABLE IV

Calculated pore radii of the bonded packings

DESIGNATION OF PACKING MATERIAL	MEASURED R_p (nm)	PORE RADII DERIVED FROM			
		S_{BET}	V_p	CHAIN VOLUME v_{sp}	CHAIN LENGTH L
RP-3	7.3	7.4	7.4	7.5	7.4
RP-10	6.6	6.8	7.1	7.0	6.6
RP-18	6.0	6.0	6.2	6.6	5.6

ness of the liquid layer is then equal to the ratio of the liquid volume and the BET-surface. In turn, the liquid volume (per gram silica) can be written as

$$v_{sp} = \nu_i \cdot N \qquad (3)$$

where N is the surface coverage (in mol/g) taken from table II a and ν_i the molar volume (in cm^3/mol) of the bonded chains calculated from data published by Fedors |34|. For RP-3, RP-10 and RP-18, v_{sp} equals 0.15, 0.26 and 0.36 cm^3/g, respectively.

Finally, the pore radii presented in the last column of table IV are derived from a model presented in figure 4. Here, the bonded chains are assumed to stand upright on the silica surface. The remaining pore radius of pure silica (i.e 8 nm) minus the chain length calculated from covalent and Van der Waals radii, taking the Si-O-Si bond angle as 130 degrees |1|. In this model we assume that the BET-surface area of pure silica is measured on top of the hydroxyl groups. The effective chain length, L, is then equal to the total length of the RP-chain minus the length of a hydroxyl group. The chain lengths, L, derived for the RP-3, RP-10 and RP-18 bonded packings are 0.56, 1.44 and 2.45 nm, respectively.

The two models considered for the bonded phases represent two limiting situations. For the densily packed liquid-like coating, the layer thickness is minimal and hence the remaining pore radius is maximal. For the upright, brush-type chains the layer thickness is maximal and thus the remaining pore radius is minimal. Indeed, the data in the final column of table IV are all smaller than the corresponding values in the last but one column.

It is more interesting to compare these two sets of data with the experimental values in the preceeding three columns. For the RP-3 phase the theoreti-

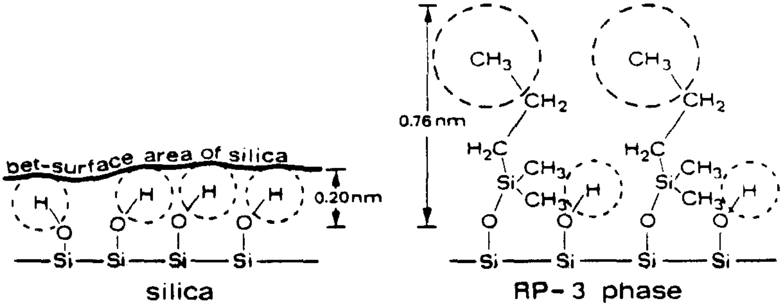

FIGURE 4
Model for calculating n-alkylsilyl bonded chain lengths

cal models show little variation, but the experimental data seem to favour a linear model. For the RP-10 phase the three experimental data vary between the two limiting values offered by the models. For the RP-18 phase the three experimental values agree quite well and fall midway between the two theoretical limits. It seems, therefore, that the smaller chains stand upright on the silica surface, whereas the longer chains are more bent and intertwined.

We, therefore, disagree with the straightforward conclusion of Unger |17,20| that all RP-chains are bonded straight to the surface. Unger derives this conclusion from the agreement between the pore radii calculated from linear chains and the values measured directly. However, his experimental data do not agree with values found from BET-surface areas and pore volumes.

The disagreement between the experimental data, on the one hand, and the pore radii derived from the phase molar volume, on the other hand, (last but one column in table IV) proves that the bonded phase does not behave as a liquid. Note that equally large pore radii, R_v^{sp}, would also be measured, if the bonded chains are completely penetrable by the nitrogen molecules. The fact that —for longer chains— the experimental data fall midway between the two sets of model data, indicate that either the chains are partially bent or that the upright chains are only partially penetrable for nitrogen. Apparently, this situation prevails under the freeze-dried conditions of the nitrogen sorption measurements (-196°C).

In fact, the dissimilarity between the chromatographic conditions and the conditions during the sorption measurements is one reason to be careful. Undoubtedly, the bonded chains will not behave rigidly at roomtemperature. Also, the hydrocarbon chains may be sensitive to the polarity of the mobile phase, such as methanol-water. In other words, bonded phases that assume an upright position in contact with liquid nitrogen at -196°C, need not do so in contact with water at roomtemperature. As will be discussed in a forthcoming paper |35|, the nonpolar chains tend to diminish their surface area in a strongly polar environment.

The main conclusion to be drawn from the data in table IV is the close agreement between the experimental pore radii on the one hand, and the theoretically calculated values on the other hand. These sets of data do not allow to make a distinction between brush-type, upright chains and intertwined, liquid-like phase.

Geometrical pore model of chemically bonded stationary phases

Since 99.9% of the specific surface area of pure silica is inside the particles, the surface coverage with bonded phase is nearly exclusively confined to the pores of the particles. Now, for cylindrical pores the surface is not flat but curved, the more so as the average pore radius of pure silica is smaller.

The data of surface coverage (table II a), pore structure and chain geometry (tables III and IV), can be collected into a pore-model for the chemically bonded phase. This model is presented in figure 5 for the RP-3, RP-10 and RP-18 phases, where it is assumed that all chains stand upright on the silica surface.

First, the mutual distance between the chains, d_{RP}, is calculated from the surface coverage by assuming the closest density of the chains on the silica surface, so that every individual chain occupies an equal hexagonal surface area. The distance between the centre of the chains is then given by

$$d_{RP} = 1.075 \cdot N^{-\frac{1}{2}} \qquad (4)$$

where d_{RP} is expressed in nm, when the surface coverage N is expressed in nm^{-2} as in table II a. The surface coverage of hydroxyl groups on the silica surface is taken as 4.8 nm^{-2}.

Next, we consider the space occupied by the chains. To this order we draw in figure 5 the calculated pore radii, $R_{V_{sp}}$ and R_L, that indicate the minimum and maximum thickness of the bonded phase layer. If, under chromatographic conditions the actual pore radius would be equal to $R_{V_{sp}}$, the bonded phase resembles a liquid of hydrocarbons.

On the other hand, if the chains are stretched perpendicurlarly to the surface, the pore radius is shortened to R_L and there is some spacing between individual chains, as shown in figure 5. Under chromatographic conditions the spacing will be filled up by mobile phase molecules because no cavities or voids can exist in a chromatographic column.

In reality, of course, the chains are not evenly distributed, but rather more randomly with some chains grouped together and other chains more widely separated. Such a random distribution has been presented previously for an RP-1 phase |1|.

If the average experimental pore radius, $\overline{R_p}$, as measured or derived from the BET-surface area and the pore volume (table IV), is a fair representation of the chromatographic practice, then it follows from figure 5 that the conditions are somewhat in between the foregoing extremes. There would be some space between the bonded chains available for penetration by mobile phase molecules.

The preceeding remarks are valid for each bonded phase, independent of its chain length. If we now compare different chain lengths, we see that the surface coverage decreases and hence the interspacing increases with increasing chain length. Consequently, for linear, brush-type chains the space between individual chains increases with chain length. The schematic molecules drawn in figure 5 show that for the RP-3 phase and -to a lesser extent- the RP-10 phase, the surface coverage is restricted by the two bulky methyl groups bonded to the silicon atom.

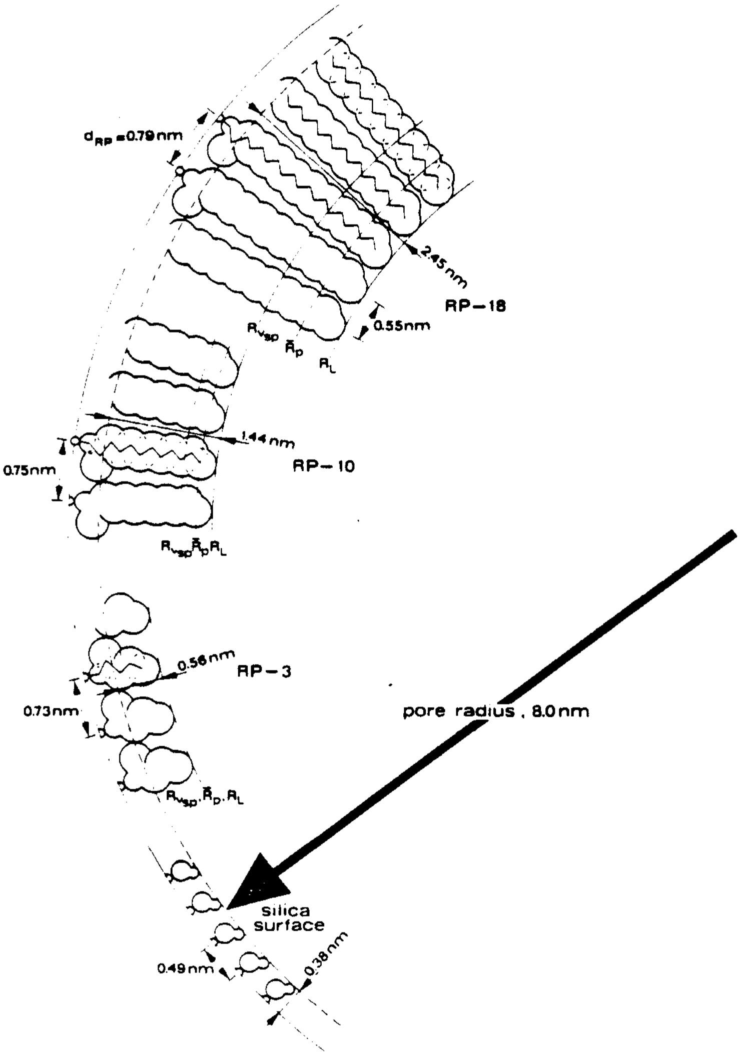

FIGURE 5

PORE MODEL FOR CHEMICALLY BONDED STATIONARY PHASES

$\bar{R}_p$ denotes average experimentally measured pore radii (table IV); $R_{v_{sp}}$ and R_L represent pore radii calculated from molar volumes and chain lengths, resp.

However, for the long RP-18 chains this is no longer true and here the maximum surface coverage is thought to be determined by the close approximation of the ends of the upright chains. This effect can only become manifest for curved surfaces as found in cylindrical pores. If true, it would mean that the pore radius of the silica support influences the surface coverages for longer chain lengths. The smaller the pore radius, the smaller the coverage will be. Reversely, for a given pore radius of the silica support, the coverage decreases with increasing chain length. Thus, the decrease in coverage is not determined by the available BET-surface area of the bare silica support, but by the area at the point where the bonded chains end.

Estimate of surface coverage

In figure 6 we have attempted to put the preceeding arguments on a quantitative basis. Here, we have plotted experimental and calculated values for the surface coverage as a function of the RP-chain length (expressed in carbon num-

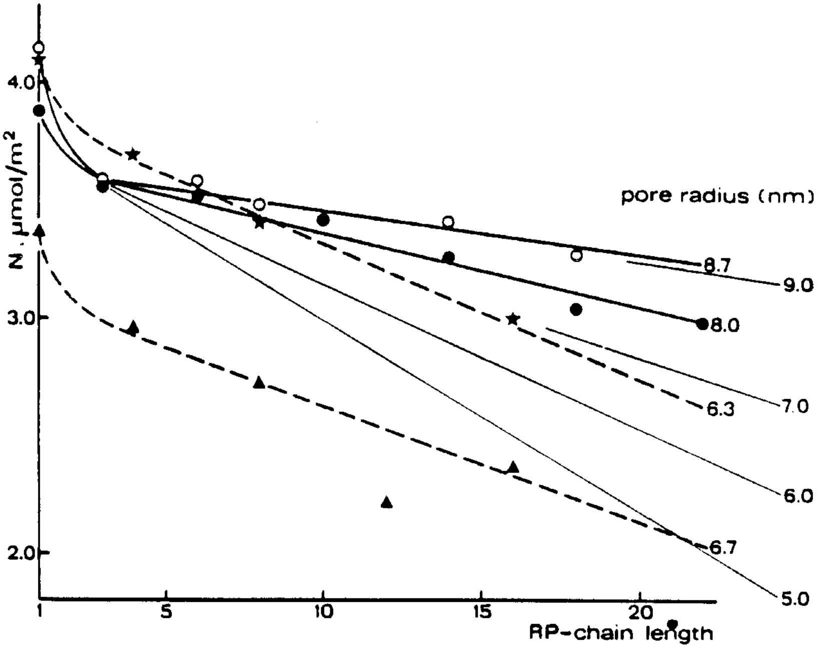

FIGURE 6

Surface coverage as a function of RP-chain length for various average pore radii of the support material. Thin solid curves are calculated as discussed in the text. Other curves refer to experimental data:

● *table II a,* ○ *table II b,* ★ *Unger et al. /16/,* ▲ *Unger et al. /17,20/*

ber) for cylindrical pores of various diameter. In the calculation we assume that long-chain molecules cover the surface to such an extent, that their ends (at length L) touch. In other words, the separation between two chains at the top is assumed to be constant. To find the corresponding interspace between two adjacent chains at the silica surface, we must multiply this constant separation with $R_p/(R_p-L)$, where R_p is the pore radius of pure silica and L the alkyl chain length. The surface coverage is inversely proportional to this factor, so that

$$N \sim (R_p - L)/R_p \tag{4}$$

Indeed, it can be seen in figure 6 that the experimental data from table II a and II b show a linear decrease of the surface coverage with increasing chain length, L, at least from RP-3 upward.

The proportionality factor is derived from the experimentally observed coverage of 2.98 μmol/m^2 for RP-22 (L = 2.95 nm) on silica with an average pore radius of R_p = 8 nm. Hence, the surface coverage with RP-22 on silicas with pores of different radius is found as

$$N_{RP-22} = \frac{R_p - 2.95}{R_p} \cdot \frac{8}{8 - 2.95} \cdot 2.98 = 4.72 \cdot (R_p - 2.95)/R_p \tag{5}$$

Finally, we assume that the coverage with RP-3 is determined by the two bulky methyl groups and independent of the pore radius. The surface coverage with intermediate chain length is then calculated by linear interpolation, between the constant coverage of 3.6 μmol/m^2 for RP-3 and the value derived from eq. (5) for RP-22. The resulting straight lines are indicated in figure 6 for average pore radii of 5, 6, 7 and 9 nm.

The higher coverages from table II b in comparison to table II a, can now be explained from the larger pore radius of 8.7 nm. Actually, the data points in figure 6 slightly exceed the theoretical line calculated for an average pore radius of 9 nm, but this can be attributed to the influence of the pore size distribution, which is not taken into account in the above analysis.

A similar comparison can be made for experimental data published by Unger et al. |16,17,20|. The data referring to a pore radius of 6.3 nm and a BET-surface area of 301 m^2/g, fall nicely in between the curves calculated for pore radii of 6 and 7 nm,respectively. By contrast, the data of Unger for a pore radius of 6.7 nm |17,20| fall short of the coverage expected for this radius, although they do show the expected decrease with chain length. We consider it likely that the disagreement arises from an erroneously measured BET-surface area. Indeed, if Unger's reported high value of 376 m^2/g is changed to a value of 315 m^2/g (compare table III), the surface coverage of an RP-4 phase would increase from Unger's value of 2.97 $\mu mol/m^2$ to 3.55 $\mu mol/m^2$, and all other data would agree better with the expected curve.

A value of 315 m^2/g for the BET-surface area of the silica support would also agree better with the BET-surface areas of Unger's bonded phases, and —when substituted into eq. (2)— yield pore radii in better agreement with directly measured values |17,20|.

The picture developed in figs. 5 and 6 provides an explanation for the presently observed decrease in surface coverage of porous silica with longer RP-chains. It is true, however, that the silicas included in this study cover only a small range in pore radius. It would be advisable to extend the observations to silica with much narrower or much wider pores. If our simplified model is correct, we would predict that the decrease in surface coverage with increasing chain length is more manifest for smaller pores. Reversely, we expect that silicas with a pore radius over 12 nm show nearly equal coverages for RP-3 up to RP 22.

The increase in surface coverage observed in fig. 6 between RP-3 (3.6 $\mu mol/m^2$) and RP-1 (about 4 $\mu mol/m^2$) is stronger than expected from eq. 4. This relatively strong increase might be attributed to the influence of smaller pores. Although micropores (<1 nm) are absent, there is a substantial fraction of pores with radii down to 3 nm. Such narrow pores are fully covered with small trimethylsilyl molecules, but only sparsely with larger alkyl silanes. Nevertheless, even such a meagre coverage prevents the small trimethylchlorosilane molecule to approach the silica surface as evidenced by the imperceptible effect of post-silanization.

Thermal stability of bonded packings

The thermal stability of several RP-packings (table II a) was tested by Thermogravimetry coupled to Mass Spectrometry (TG-MS). In this combination the thermogravimetric apparatus acts as the sample source for the Mass Spectrometer. During the gradual increase of the temperature the decomposition can be closely watched with the MS. Two different experiments were performed to determine the temperature at which decomposition starts.

The first experiment was performed under vacuum. From the measurements it appears that decomposition of all RP-packings starts between 305 and 320°C. The same temperature-range was found by Rehâk and Smolková |36|, whereas Van de Venne found 250°C |19|. These investigators only applied Thermogravimetry and conclude that the bonds between silicon and carbon are broken sooner than the Si-O-Si bonds. Unger |20| agrees with this opinion on the basis of a comparison between the bond energies of C-C, Si-C and Si-O, i.e. 348, 306 and 444 kJ/mol, resp.

Our data do not confirm this. As an example, figure 7 presents MS-spectra for a RP-10 bonded packing subjected to two different temperatures. Obviously, decomposition starts at 310°C and is much more pronounced at 420°C. Note, that both spectra show the same fragment ions. Particularly noteworthy are the small peak at m/e 199 corresponding to $Si(CH_3)_2C_{10}H_{21}$, and the peak at m/e 74 corresponding to $OSi(CH_3)_2$. The presence of these peaks in both spectra indicates that the Si-O-Si bond is already ruptured at a relatively low temperature of 300°C. There is no indication that the Si-C bond is ruptured before the Si-O-Si bond. Possibly, the linkage of the Si-O-Si bond between the inorganic silica and an organic moiety reduces its bond-strength below the value of 444 kJ/mol quoted by Unger |20|.

Another experiment was performed in air with an RP-14 packing. At a temperature of 205°C a CO_2-peak quickly starts to grow. Only small fragment ions (< m/e 85) are observed in very small amounts. No fragment ions with mass 74 appear. This indicates that the chains burn off under these conditions. Thus, bonded materials from which samples are taken for elemental analysis or which

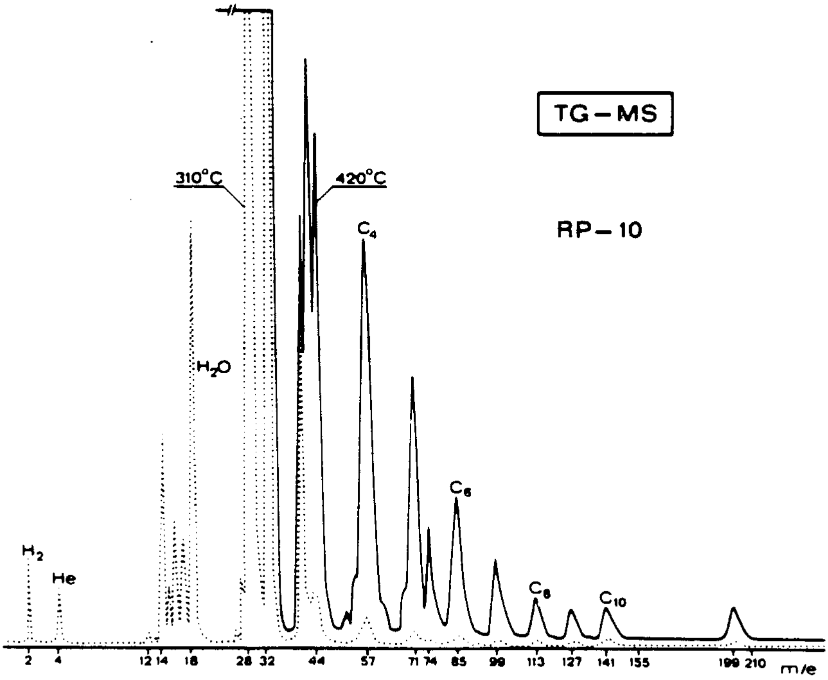

FIGURE 7

Mass spectra of material released from an n-decyldimethylsilyl bonded phase at two temperatures (during a thermogravimetric run) are subjected to post-silanizating with a small silylating agent, may not be dried over 150°C (in air).

CONCLUSIONS AND RECOMMENDATIONS

Chemically bonded stationary phases can be easily and reproducibly be synthesized with relatively high surface coverages independent of the type of bonded phase (with or without a functional end-group). With monochlorosilanes higher surface coverages are reached than with monoalkoxysilanes under equal conditions.

The necessary monochloro- and monoalkoxysilanes can be easily synthesized by a very simple one-step catalytic hydrosilylation reaction of olefins, providing a high yield of 80%.

Chemically bonded phases prepared at roomtemperature (in an erlenmeyer) showed a slightly lower surface coverage (∿0.2 μmol/m^2) than those prepared at a higher temperature (∿100°C).

Provided the bonding reaction is run to completion, post-silanization (e.g. with trimethylchlorosilane) does not enhance the carbon percentage and leave the chromatographic properties unaffected, at least under reversed phase conditions.

Thermogravimetry - Mass Spectrometry data indicate that not only the Si-C bond, but all bonds in the bonded n-alkyldimethylsilyl chain, including the Si-O bond, start to break at 310°C *in vacuo*. In air the alkyl chain starts to burn off at 205°C.

Physical adsorption measurements provide a clear and consistent picture of the pore structure of silica. In LiChrosorb SI 100, which forms the support material in the present study, micropores (<1 nm) are absent and all pores are cylindrically shaped with pore radius, BET-surface area and pore volume consistently decreasing with increasing length of the bonded hydrocarbon chain. Shorter chains stand approximately upright on the silica surface. Longer chains are more closely packed, but never as closely as the corresponding liquid phase.

The data on pore radius and surface coverage can be collected into a geometrical model for the bonded chains. For very short chains (up to three carbon atoms), the maximum coverage is determined by the closest possible approach of the methyl groups bonded to the silicon atom. This coverage is thus independent of the type of silica (provided that enough reactive silanol groups are available) and amounts to about 4.0 μmol/m^2 for RP-1. For longer chain lengths the coverages depend upon the pore radius of the silica support. The longer the chain and the smaller the pore radius, the more the coverage decreases, and consequently the more bare silica surface remains, and with that remaining silanol groups. Consequently, if accessible, the latter influence the retention of polar, and particularly basic substances |37|.

The same type of bonded packing prepared from two batches with different pore size, may yield different retentions due to a difference in the ratio of silanol groups to bonded chains. If the average pore radius of a given silica support is known, coverages can be estimated for every chain length. A pore radius of about 12 nm is estimated as a radius at which equal coverages of about 3.6 $\mu mol/m^2$ can be reached for chain lengths up to RP-22. As an exception, the RP-1 phase always shows a slightly higher surface coverage of about 4.0 $\mu mol/m^2$, which enhancement must be caused by the smaller pores (>1 nm) in the silica support.

For a silica support with a pore radius of 8 nm coverages were obtained of 3.9 $\mu mol/m^2$ for the RP-1, decreasing to 3.0 $\mu mol/m^2$ for an RP-22 bonded packing.

This analysis would not have been possible from the limited information provided with commercial silicas or bonded phase packings. It required extensive adsorption measurements with physical instrumentation not available to every laboratory. Consequently, we consider it essential that the information provided by manufacturers becomes more detailed and more accurate. The more so as we and others |19| have noted that the value stated for the (average) pore size of the silica support does not agree with measured values. We suspect that such data are not measured for each batch separately, but are simply a repetition of earlier values, possibly referring to a quite different silica batch.

According to Karger and Giese there is a growing awareness about the quality of the bonded packings. Their overall performance can be improved, particularly with respect to efficiency, stability and reproducibility in retention and selectivity |37|.

We believe that the technology of making ideal silica supports is not yet available so that every silica batch yields a (slightly) different chemically bonded packing, which may introduce differences in retention and selectivity. This emphasizes the need for as much information as possible.

In order to fully describe a chemically bonded phase and a commercial packing, the following quantities should be provided for each individual batch.

(i) *macro properties of silica support*

- the mean value and the distribution of the particle size
- the particle shape (regular/irregular)

(ii) *micro properties of silica support*

- the specific surface area of the original silica support (S_{BET} in m^2/g)
- the average pore radius of the original silica support in order to estimate whether the geometrical maximum surface coverage is reached

- the pore size distribution of the original silica support for uniformity (are micropores present?)
- the pore shape
- the pore volume of the original silica support, which can be used for the calculation of the column porosity |35|

(iii) chemical modification

- since the carbon percentage is not sufficiently specific, the silane reagent used in the bonding reaction must be specified. Only then the bonding type and the surface coverage can be derived.
- the results of elemental analysis in weight percent per gram modified silica. If the bonded material is post-treated with trimethylchlorosilane the percentages should be given before and after post-silanization (especially important when dichloro- and trichlorosilanes are used). Carbon data are of primary interest but should be corroborated with results for hydrogen and hetero-elements, if present.

With these quantities the surface coverages (N in $\mu mol/m^2$) can be calculated and, assuming that the surface density of hydroxyl groups is approximately 4.8 per nm^2, the ratio of silanol groups to bonded chains.

ACKNOWLEDGEMENTS

The authors thank Mr. A. van Pelt for carefully synthesizing a number of the chemically bonded phases; Ir. C. Olieman of the Laboratory for Organic Chemistry for his helpful comments during the preparation of the chemically bonded phases, and Ir. B. Don of the Laboratory for Physical and Anorganic Chemistry for his advice and the measurement of the physical adsorption data. The assistance of Dr. Ir. G. Hakvoort during the TG-MS measurements was greatly appreciated. Mr. P.C. Steyne and Mr. A.P.E. Maljaars of the Laboratory for Chemical Technology, and Mr. W.J. Buis of the Institute for Organic Chemistry TNO are gratefully acknowledged for the high precision data on elemental composition.

REFERENCES

1. Berendsen, G.E. and Galan, L. de, *J. Liquid Chromatogr.*, 1, 403, 1978
2. Berendsen, G.E. and Galan, L. de, *J. Liquid Chromatogr.*, 1, 561, 1978
3. Majors, R.E. and Hopper, H.J., *J. Chromatogr.*, 12, 767, 1974

4. Gilpin, R.K., Korpi, J.A. and Janicki, C.A., *Anal. Chem.*, 46, 1314, 1974

5. Knox, J.H. and Pryde, A., *J. Chromatogr.*, 112, 171, 1975

6. Kirkland, J.J., *Chromatographia*, 8, 661, 1975

7. Kingston, D.G.I. and Gerhart, B.B., *J. Chromatogr.*, 116, 182, 1976

8. Kikta, E.J. and Grushka, E., *Anal. Chem.*, 48, 1098, 1976

9. Karch, K., Sebestian, I. and Halász, I., *J. Chromatogr.*, 122, 3, 1976

10. Hemetsberger, H., Maasfeld, W. and Ricken, H., *Chromatographia*, 9, 303, 1976

11. Hemetsberger, H., Kellerman, M. and Ricken, H.,*Chromatographia*,10, 726, 1977

12. Little, C.J., Dale, A.D. and Evans, M.B., *J. Chromatogr.*, 153, 381, 1978; 153, 543, 1978

13. Hennion, M.C., Picard, C. and Caude, M., *J. Chromatogr.*, 166, 21, 1978

14. Little, C.J., Dale, A.D., Evans, M.B. and Whatley, J.B., *J. Chromatogr.*, 171, 431, 1978; 171, 435,1978

15. Hemetsberger, H., Behrensmeyer, P.,Henning, J. and Ricken, H., *Chromatographia*, 12, 71, 1979

16. Unger, K.K., Becker, N. and Roumeliotis, P., *J. Chromatogr.*, 125, 115, 1976

17. Roumeliotis, P. and Unger, K.K., *J. Chromatogr.*, 149, 211, 1978

18. Tanaka, N., Goodell, H. and Karger, B.L., *J. Chromatogr.*, 158, 233, 1978

19. Venne, J.L.M. van de, *Thesis*, Eindhoven University of Technology, Wibro, Helmond, The Netherlands, 1979

20. Unger, K.K., *Porous Silica*, J. Chromatogr. Library, Vol.16, Elsevier, Amsterdam, 1979

21. Colin, H. and Guiochon, G., *J. Chromatogr.*, 141, 289, 1977

22. Brunauer, S., Emmett, P.H. and Teller, E., *J. Amer. Chem. Soc.*, 60, 309, 193

23. Boer, J.H. de, in *The Structure and Properties of Porous Materials*, edited b D.H. Everett and F.S. Stone, Butterwoths, London 1958, p. 68

24. Broekhoff, J.C.P., *Adsorption and Capillarity*, *Thesis*, Delft University of Technology, Waltman, Delft, The Netherlands, 1969

25. Linsen, B.G., *Physical and Chemical Aspects of Adsorbents and Catalysts*, Academic Press, London, 1970

26. Seyferth, D. and King, R.B., *Organometallic Chemistry Reviews*; Annual Survey Silicon - Germanium - Tin - Lead; Elsevier, Amsterdam, 1978, p.11 - 16

27. Boksányi, L., *Thesis no. 200*, Ecole Polytechnique Federale de Lausanne, Clausthal - Zellerfeld, Bönecke-Druck, 1975

28. Oswald, A.A., Murrel, L.L. and Boucher, L.J., *Prep. Div. Pet. Chem. Am. Chen Soc.*, 19, 155, 1974

29. Voronkov, M.G., Tsykhanskaya, I.I., Vlasova, N.N., Kaliberdo, L.M., Gont, L Korotaeva, I.M. and Satsuk, E.I., *Izv. Akad. Nauk. SSSR, Ser. Khim.*,1368,19

30. Mourey, T.H. and Siggia, S., *Anal. Chem.*, 51, 763, 1979

31. Lippens, B.C., Linsen, B.G. and Boer, J.H. de, *J. Catal.*, 3, 32, 1964

32. Lippens, B.C. and Boer, J.H. de, *J. Catal.*, 4, 319, 1965

33. Boer, J.H. de, Linsen, B.G. and Osinga, Th.J.O., *J. Catal.*, 4, 643, 1965

34. Fedors, R.F., *J.P.L. Quarterly Technical Review*, 3, 45, 1973

35. Berendsen, G.E., Schoenmakers, P.J., Galan, L. de, Vigh, Gy., Varga-Puchony, Z. and Inczédy, J., *J. Chromatogr.*, submitted for publication

36. Rehák, V. and Smolková, E., *Chromatographia*, 9, 219, 1976

37. Karger, B.L. and Giese, R.W., *Anal. Chem.*, 50, 1048A, 1978